

## Accepted Manuscript

Title: Study on glutathione's inhibition to dopamine polymerization and its application in dopamine determination in alkaline environment based on silver selenide/molybdenum selenide/glassy carbon electrode

Author: Xiaohong Xia Xuan Shen Yonglin Du Weichun Ye Chunming Wang



PII: S0925-4005(16)31016-4  
DOI: <http://dx.doi.org/doi:10.1016/j.snb.2016.06.154>  
Reference: SNB 20480

To appear in: *Sensors and Actuators B*

Received date: 10-5-2016  
Revised date: 20-6-2016  
Accepted date: 27-6-2016

Please cite this article as: Xiaohong Xia, Xuan Shen, Yonglin Du, Weichun Ye, Chunming Wang, Study on glutathione's inhibition to dopamine polymerization and its application in dopamine determination in alkaline environment based on silver selenide/molybdenum selenide/glassy carbon electrode, *Sensors and Actuators B: Chemical* <http://dx.doi.org/10.1016/j.snb.2016.06.154>

This is a PDF file of an unedited manuscript that has been accepted for publication. As a service to our customers we are providing this early version of the manuscript. The manuscript will undergo copyediting, typesetting, and review of the resulting proof before it is published in its final form. Please note that during the production process errors may be discovered which could affect the content, and all legal disclaimers that apply to the journal pertain.

**Study on glutathione's inhibition to dopamine polymerization and its application  
in dopamine determination in alkaline environment based on silver  
selenide/molybdenum selenide/glassy carbon electrode**

Xiaohong Xia, Xuan Shen, Yonglin Du, Weichun Ye, Chunming Wang<sup>\*</sup>

School of Chemistry and Chemical Engineering, Lanzhou University, Lanzhou, 730000, P. R.

China

---

<sup>\*</sup> Corresponding author. Tel.: +86 9318911895; fax: +86 9318912582.  
E-mail address: wangcm@lzu.edu.cn (C. Wang)

**Highlights:**

- Cysteiny residue of glutathione is the action target for dopamine quinone.
- Glutathione inhibited dopamine polymerization in alkaline environment successfully.
- This inhibition realized the oxidation of dopamine with lower energy consumption.
- Based on glutathione, dopamine determination in alkaline environment was realized.
- This biosensor displays high sensitivity and stability for dopamine determination.

## **Abstract**

Cellular glutathione plays critical roles in protecting neuronal cells against dopamine induced oxidative stress and electrophilic cellular damage; inspired by above mentioned properties of glutathione, we used glutathione as a polymerization inhibitor to develop a dopamine biosensor which can be used in alkaline environment. The detection of dopamine in alkaline environment has been challenged by its polymerization for many years, glutathione as a kind of thiol can be used to prevent the polymerization of dopamine in alkaline environment by eliminating the electrophilic quinone molecules needed during the polymerization. In order to enhance the electrochemical performance of electrode, Ag<sub>2</sub>Se/MoSe<sub>2</sub> composite with large exposed surface areas was synthesized, which improved the sensitivity and stability for dopamine detection. The low oxidation peak potential for dopamine, 0.04 V vs. SCE, indicates that glutathione can realize the electrooxidation of dopamine at lower potential in alkaline environment. In this study, by introducing glutathione to inhibit the dopamine polymerization, sensitive and stable detection of dopamine can be achieved at pH 8.5 based on the Ag<sub>2</sub>Se/MoSe<sub>2</sub>/GCE.

## **Keywords:**

Glutathione; Polymerization inhibitor; Silver/molybdenum selenide; Dopamine sensor; Alkaline environment

## **1. Introduction**

Parkinson's disease caused by selective loss of dopaminergic neurons in the substantia nigra results in the reduction of the dopamine (DA) levels in the striatum [1-3]; it is characterized by the motor deficits including the resting tremor, bradykinesia, rigidity, and impairment of postural reflexes [4-6]. Among various pathological signs of Parkinson's disease, oxidative stress is one of the major factors which could exacerbate the patient's condition [7,8]. Previous reports indicate that one of the reasons to produce oxidative stress is the imbalance of DA metabolism, which results in the proliferated production of reactive oxygen species and the consequent oxidative/electrophilic stress, as well as mitochondrial dysfunction, leading to the mitochondrial dysfunction [9-12]. To minimize the oxidative/electrophilic damage, cells have evolved lots of antioxidants. For example, the cellular glutathione (GSH) is demonstrated to play critical roles in protecting neuronal cells against DA induced oxidative stress and electrophilic cellular damage [13,14]. GSH can react with electrophilic quinone molecules and reactive oxygen species to minimize DA induced neurocytotoxicity, GSH alteration is precede loss of dopaminergic neurons as well as accumulation of "Lewy bodies" in Parkinson's disease patients, and it is directly related to severity of Parkinson's disease [15]. In fact, alterations of cellular GSH in substantia nigra have been described as biochemical characteristics of Parkinson's disease, the levels of total as well as reduction of GSH are significantly depleted in the substantia nigra pars compacta of Parkinson's disease patients [16,17]. The reactive oxygen species/free radicals which can lead to the mitochondrial dysfunction

and exacerbate the patient's condition is resulting from DA oxidation or enzyme degradation metabolism, and which can be eliminated by GSH. Based on above medical research, an idea is sprouted; the special property of GSH mentioned here can be used to prevent the polymerization of DA in alkaline environment. If this favorable anticipation can be realized, the challenge, detection of DA in alkaline environment, which has puzzled researchers for years, will be solved perfectly.

To date, the DA determination has been carried out using conventional analytical techniques including surface-enhanced raman scattering [18,19], fluorescence [20], self-powered triboelectric nanosensor [21], NMR relaxation method [22], colorimetric sensor [23], capillary electrophoresis [24], and spectrophotometry [25]. Electrochemical methods have appeared to be suitable and more often employed in the clinical analysis to determine the concentration of DA owing to easy operation, cost effectiveness, and it provide enough sensitivity to real time monitoring of the analytes [26-28]. Nonetheless, electrochemical observation of DA under physiological conditions is a challenging issue because its presence in the biological fluids is extremely low compared to ascorbic acid (AA) and uric acid (UA) and their oxidation potentials are extremely close in physiological media (pH 7.4). And worse still, the oxidized form of DA can accelerate the oxidation of AA resulting in the poor selectivity of biosensors [29-33]. Hence, the elimination of the interference caused by these species is very crucial as the overlapped voltammetric signal can result in the fouling effects and poor selectivity of electrode. To overcome the influence of these factors, some researchers try to determine DA under alkaline environment; however,

the problem is the polymerization of DA in alkaline environment [34-36]. The DA polymerization in alkaline environment can cause lower sensitivity and stability for DA detection. Therefore, there are some works focused on transition-metal dichalcogenides. Layered transition-metal dichalcogenides are very fascinating in electrocatalysis and biosensing in terms of good electronic and electrochemical properties [37]. Material with special morphology has shortened path lengths for ions diffusion and large exposed surface areas, which play important roles in enhancing the electrochemical performance [38]. Among the many transition-metal dichalcogenides, metal selenide might be a good choice for electrochemical application [39]. Reports show that MoSe<sub>2</sub> has higher intrinsic electrical conductivity than MoS<sub>2</sub> due to the more metallic nature of Se [40, 41]. In recent years, the application of MoSe<sub>2</sub> in electrochemical sensing is very popular. For example, Huang et al. successfully synthesized aptamer/Au nanoparticles/cobalt sulfide nanosheets biosensor for 17 $\beta$ -estradiol detection using a guanine-rich complementary DNA sequence for signal amplification [42].

In this work, GSH was used as the polymerization inhibitor which can effectively prevent the polymerization of DA in alkaline environment. In addition, the oxidation potential of DA linearly shifted in negative direction with increasing pH of the solution; the oxidation potential is closely related to the energy needed to oxidize the target analyte, lower oxidation potential means lower energy requirement. So increasing pH of the solution also can be considered as a way to reduce the energy requirement during the precise monitoring of DA in alkaline environment. Despite the

performances of above mentioned polymerization inhibitor, improving the electrocatalytic properties of substrates for highly sensitive and target selective sensing is still considered as a challenge for bioanalytical research and medical diagnosis. In this study, hollow spherical  $\text{Ag}_2\text{Se}/\text{MoSe}_2$  selected as the modifies because its excellent electrochemical selectivity and stability, the electrochemical property of different electrode toward DA was studied as Fig. S1. Based on the polymerization inhibitor GSH and electrode modifies  $\text{Ag}_2\text{Se}/\text{MoSe}_2$ , the highly sensitive and selective electrochemical detection for DA is achieved.

## 2. Experiment part

### 2.1. Chemicals

Hydrazine hydrate, potassium ferricyanide ( $\text{K}_3\text{Fe}(\text{CN})_6$ ), and potassium ferrocyanide ( $\text{K}_4\text{Fe}(\text{CN})_6$ ) were purchased from Shanghai Chemical Reagent Co. Ltd. Ammonium molybdate tetrahydrate ( $(\text{NH}_4)_6\text{Mo}_7\text{O}_{24}\cdot 4\text{H}_2\text{O}$ , analytically pure) and selenium powder (Se) were purchased from Aladdin.  $\text{AgNO}_3$ , DA, AA and UA were obtained from Alfa Aesar. GSH was purchased from Sigma-Aldrich, Ltd. The phosphate buffer solution (0.2 M) was prepared from  $\text{Na}_2\text{HPO}_4$  and  $\text{NaH}_2\text{PO}_4$ , the pH was adjusted regularly with NaOH. Ultrapure water (resistivity of 18.25 MV cm) was used throughout the work.

### 2.2 Preparation of $\text{Ag}_2\text{Se}/\text{MoSe}_2$

The precursor  $\text{MoO}_3$  and  $\text{MoSe}_2$  were prepared under a conventional hydrothermal reaction as implemented in supporting information. The synthesis process of  $\text{Ag}_2\text{Se}/\text{MoSe}_2$  was described as follows: 5 mL of 0.05 M  $\text{AgNO}_3$  solution



was added to the prepared MoSe<sub>2</sub> aqueous dispersion (0.05g/10 mL); then, 11 mL 0.05 M AA was gradually added with stirring. The products were separated from the solution by centrifugation, and the un-reacted species were removed by multiple washing steps with ultrapure water.

### 2.3. Characterization

The morphology of the material was investigated by scanning electron microscopy (SEM, J4800 Japan) and transmission electron microscopy (TEM, Tecnai G2 F30, FEI, USA). The phase structures of the samples were measured by X-ray diffraction (XRD, Rigaku D/max-2400, Cu K radiation). The chemical composition and valence state of these samples was determined by X-ray photoelectron spectroscopy (XPS, ESCALAB250xi X-Ray Monochromatisation 200W Spot/power: Mono 650µm). Raman was carried out using a HORIBA Jobin Yvon LabRAM HR 800. The electrochemical experiments were carried out in an electrochemical cell with a three-electrode configuration with a CHI660C electrochemical workstation (CHI, USA). Material modified glassy carbon electrode (GCE) as the working electrode, the Pt wire and saturated calomel electrode (SCE) served as the counter electrode and reference electrode, respectively.

### 2.4 Research method for polymerization inhibition of GSH

The inhibition performance of GSH on DA polymerization was researched using Ag<sub>2</sub>Se/MoSe<sub>2</sub>/GCE in alkaline environment. The electrochemical cyclic voltammetry (CV) and electrochemical impedance spectra (EIS) were employed to study the changes in the electrochemical properties of electrode surface before and

after the presence of GSH. The SEM was employed to study the changes in the morphology of electrode surface before and after the presence of GSH. Raman measurements were carried out to confirm the generation of polydopamine and the inhibition property of GSH on DA polymerization in alkaline environment.

### 3. Results and discuss

#### 3.1. Structure characterization of $\text{Ag}_2\text{Se}/\text{MoSe}_2$

As shown in Fig. 1a, the regular spherical structure of this prepared  $\text{Ag}_2\text{Se}/\text{MoSe}_2$  can be observed, the radius of these spheres is about 250 nm. The TEM image shown in Fig. 1b displays that there are some particles with a radius of 15 nm attach onto the sphere surface. As shown in Fig. 1c, the high resolution transmission electron microscopy (HRTEM) image of the sphere surface displays two sets of crystal lattice fringes with spacing of 0.33 and 0.27 nm, corresponding to the in-plane lattice parameters of the  $\text{MoSe}_2$  monolayer and the interplanar distances of (200) planes, respectively [43]. The HRTEM image of the nanoparticles attached on sphere surface shows a well-defined crystal structure with the lengths of the lattice spacing is about 0.31 and 0.26 nm, corresponding to the (121) planes of orthorhombic  $\text{Ag}_2\text{Se}$  [44]. Fig. 1d and e show the fast fourier transform (FFT) pattern of the selected areas marked by frame A and B, respectively. Fig. 1f displays the XRD pattern of  $\text{Ag}_2\text{Se}/\text{MoSe}_2$ . The diffraction peak marked with diamond corresponding to the (110) reflections of  $\text{MoSe}_2$  [45], and the diffraction peak (120), (121) and (201) marked with asterisks originating from the orthorhombic  $\text{Ag}_2\text{Se}$  phase [46].

The Mo 3d XPS spectrum shown in Fig. 2a displays a perfect fit to the two peaks

located at 228.8 and 231.9 eV, corresponding to the Mo 3d<sub>5/2</sub> and Mo 3d<sub>3/2</sub> of molybdenum in a formal 4<sup>+</sup> oxidation state [47]. Fig. 2b shows the XPS spectrum of Ag 3d, the peaks centered at 367.8 and 373.8 eV correspond to the Ag 3d<sub>5/2</sub> and Ag 3d<sub>3/2</sub> of Ag<sub>2</sub>Se [48]. As shown in Fig. 2d, the BE of O 1s, 532.7 eV correspond to the chemically absorbed oxygen site [49,50]. As shown in Fig. 2c, the BE doublet located at 53.4 and 54.7 eV corresponding to the Se 3d<sub>5/2</sub> and Se 3d<sub>3/2</sub> originated from the Se<sup>2-</sup> in MoSe<sub>2</sub> [47]; the BE peak located at 54.1 eV corresponding to the Se 3d<sub>5/2</sub> is attributed to the Se<sup>2-</sup> in Ag<sub>2</sub>Se [48].

### 3.2. Inhibition of GSH on DA polymerization

The electrochemical property of different electrode toward DA was studied as Fig. S1a. Ag<sub>2</sub>Se/MoSe<sub>2</sub>/GCE exhibited higher activity for DA electro-oxidation than others, the peaks located at 0.06 V and -0.13 V vs. SCE correspond to the oxidation of DA to dopamine-o-quinone and the reduction of dopamine-o-quinone; the peak located at -0.75 V vs. SCE correspond to the reduction of oxygen. The conductivity of various electrodes have also been studied as Fig. S1b shows. In order to study the inhibition of GSH on DA polymerization, first we should find out the polymerization conditions of DA. Continuously CV scanning in DA solution at different pH (Fig. S2a, d and g) was measured to study the impact of pH value on DA oxidation, the CVs (Fig. S2b, e and h) and EIS (Fig. S2c, f and i) in K<sub>3</sub>[Fe(CN)<sub>6</sub>]/K<sub>4</sub>[Fe(CN)<sub>6</sub>] solution were measured to study the changes of electrode surface during continuously CV scanning in DA solution at different pH. The results shown in Fig. S2 indicate that the electrochemical activity and conductivity of Ag<sub>2</sub>Se/MoSe<sub>2</sub>/GCE decreased with the

increase of scan cycle and pH value. In order to study the change of electrode more directly and intuitively, the electrode surface was studied by SEM as shown in Fig. S3. After scanning in DA solution at various pH the electrode surface changed obviously after 10 cycles. It can be seen from Fig. S3b, c and d that the blur caused by films covering became more obvious with increasing pH value. During continuously CV scanning in DA solution at pH 8.5, there are some brown flocculent precipitate (inset shown in Fig. 3a) generated on electrode surface. This generated brown flocculent precipitate was characterized by Raman as Fig. 3a shows. It can be obtained from the Raman spectra that the brown flocculent precipitate generated during continuously scanning is polydopamine [51]. The polymerization of DA easy to incur in alkaline environment to produce polydopamine, before polymerization, the DA need to be oxidized into quinine and then 5,6-dihydroxyindole was produced via rearrangement. Finally, 5,6-Dihydroxyindole was polymerized to form polydopamine [51]. Based on above views the probable mechanism of dopamine polymerization was shown in Fig. 3b.

In order to study the inhibition of GSH on the DA polymerization in alkaline environment, the typical CVs of the  $\text{Ag}_2\text{Se}/\text{MoSe}_2/\text{GCE}$  recorded in 1.0 mM DA solution (pH 8.5) without and with 1.0 mM GSH are shown in Fig. 4a. It can be seen from the CV curve obtained in the DA solution, the peaks located at 0.06 V and -0.13 V vs. SCE correspond to the oxidation of DA to dopamine-o-quinone and the reduction of dopamine-o-quinone. Compared with the CV curve obtained in the DA solution without GSH, the CV curve obtained in the DA solution with GSH had

hardly changed, both of them overlapped almost completely. Above results show that the presence of GSH in DA solution could not interfere with the electrochemical reaction of DA. The role of GSH in this study is to prevent the polymerization of DA in alkaline environment, it would demonstrated by continuously CV scanning. For the DA solution without GSH (Fig. 4b), the oxidation current of DA decreased from 58.17 to 22.68  $\mu\text{A}$ , decaying to 38.99% of its initial value after 10 cycles; however, for the DA solution with GSH (Fig. 4c), the sensor retained 96.49% of its initial response after 10 cycles. In addition, during the continuously CV scanning, the color of the DA solution with GSH almost keep unchanged (inset shown in Fig. 4c); however, the color of the DA solution without GSH changed from colorless to brown (inset shown in Fig. 4b). Comparing the changes in peak current and solution color, it can be seen that GSH can prevent the polymerization of DA in alkaline environment without interfering its oxidation. In order to study the inhibition of GSH on DA polymerization in alkaline environment (pH 8.5) more directly, the morphology change of electrode surface was studied by SEM. By comparing the electrode surface shown in Fig. 4d and e it can be seen that after scanning in the DA solution without GSH for 10 cycles, the morphology of electrode surface, nanoparticles attached spheres, became blurred; it seems like some films covered the electrode surface. However, comparing the electrode surface shown in Fig. 4d and f, it can be seen that after scanning in the DA solution with GSH for 10 cycles, the morphology of electrode surface is almost no change; the nanoparticles attached spheres are still clear. The morphology changes of electrode surface shown in Fig. 4d-f make the inhibition

of GSH on DA polymerization more intuitive to understand. As the media to prevent the polymerization of DA in alkaline environment, the content of GSH is an important factor for the detection of DA in alkaline environment. The mole ratio between DA and GSH was discussed by CV as Fig. S4 shows, the optimal mole ratio between DA and GSH was determined to be 1:1.

Cysteiny residues is the action target for catechins class quinone [52,53], GSH as an tripeptide which contains cysteiny residues can react with dopamine quinone effectively. Based on above understanding, the GSH can effectively prevent the polymerization of DA because it can eliminate the electrophilic quinone molecules which resulted from DA oxidation or enzyme degradation metabolism, preventing the polymerization of DA in alkaline environment. Combining the theories about cysteiny residues and catechins class quinone with the mechanism of dopamine polymerization shown in Fig. 3b, the probable mechanism of GSH effects on the DA polymerizationv was shown in Fig. 5.

### 3.3. Electrochemical sensing performance for DA detection.

Above studies show that the GSH can be used to realize the DA detection in alkaline environment. Before the quantitative determinations, the dependence of the electrochemical oxidation of DA on pH value and scan rate was investigated as supporting information shows. Fig. S5 displays the optimal pH for electrochemical measurements in this study and Fig. S6 indicates that the oxidation of DA at  $\text{Ag}_2\text{Se}/\text{MoSe}_2/\text{GCE}$  is a typical diffusion-controlled process.

Different electrochemical methods including DPV and chronoamperometry were

employed to detect DA in alkaline environment. Fig. S7a shows the DPV curves recorded for Ag<sub>2</sub>Se/MoSe<sub>2</sub>/GCE to the successive addition of DA in PBS+GSH solution (pH 8.5). The oxidation current increased with the concentration of DA, and the dependence of the oxidation peak current ( $I_{pa}$ ) on the concentration of DA (C) was shown as curve (a) in Fig. S7c. The natural logarithm of  $I_{pa}$  ( $\log I_{pa}$ ) increased linearly with the natural logarithm of DA concentration ( $\log C$ ) in the range of 0.7 to 189.4  $\mu$ M (Fig. S7d). The linear regression equation is expressed as  $y=0.8983x-0.10530$ , and the limit of detection was calculated to be  $2.3 \times 10^{-7}$  M (S/N=3). For comparison, the DPVs recorded for Ag<sub>2</sub>Se/MoSe<sub>2</sub>/GCE to the successive addition of DA in PBS solution (pH 8.5) were also studied as Fig. S7b shows. The dependence of the  $I_{pa}$  on the concentration of DA was shown as curve (b) in Fig. S7c, and there is no linear relationship can be observed between the  $I_{pa}$  and concentration of DA. Above results show that compared with the DA response in PBS solution, the DA response on Ag<sub>2</sub>Se/MoSe<sub>2</sub>/GCE in PBS+GSH solution presented a wider linear detection range, and the polymerization inhibition of GSH is necessary for the electrochemical oxidation of DA in alkaline environment.

Typical amperometric response curves for successive injections of different concentrations of DA at steady intervals of 50 s was recorded at 0.04 V vs. SCE, the applied buffer is PBS (pH 8.5) and the test temperature is room temperature. The amperometric response curves shown in Fig. 6a and b are obtained at Ag<sub>2</sub>Se/MoSe<sub>2</sub>/GCE in PBS+GSH and PBS solution, respectively. The insetted curves in Fig. 6a and b are the details with enlarged scale of amperometric responses at low

concentration, corresponding to the parts marked by red box in Fig.6a and b. As shown in Fig. 6a, when the DA solution with different concentration was added in PBS+GSH solution (pH 8.5), the Ag<sub>2</sub>Se/MoSe<sub>2</sub>/GCE instantly responded to the analyte with the well defined, stable and steeply increased amperometric current response. The oxidation reaction occurred at the Ag<sub>2</sub>Se/MoSe<sub>2</sub>/GCE was fast in reaching the dynamic equilibrium, producing a steady state current within 1.5 s. As shown in Fig. 6c, for the Ag<sub>2</sub>Se/MoSe<sub>2</sub>/GCE response in PBS+GSH, a well defined amperometric response was observed upon each addition of DA solution, and the logI<sub>pa</sub> increased linearly with the logC of DA over the range of 0.05 to 1110 μM. The linear regression equation was expressed as  $y=0.7665x-1.340$ , with a correlation coefficient of 0.9991. The detection limit was calculated to be  $9.3 \times 10^{-9}$  M based on the 3 of the blank signals. The amperometric current responses of DA in PBS solution (pH 8.5) were analyzed and compared with that in PBS+GSH. As shown in Fig. 6b, the electrode responded to the analyte with stable and steeply increased amperometric current response at low DA concentration. The oxidation reaction occurred at the electrode produce a steady state current within 4.5 s. But then, after about 700 s, the amperometric current response began to gradually decay and this decay increased with the detection time. As a result, after a certain amount of time, the amperometric current response at higher concentration is lesser than that at lower concentration. Above results indicate that the high sensitive and wider linear determination of DA in alkaline environment could not be realized without GSH.

AA and UA usually coexist with DA in the biological fluids, the elimination of



the interference caused by them is very crucial as their oxidation potentials are almost similar. Hence, the selectivity of fabricated sensor against the analytes AA and UA with the successive addition of analytes was evaluated and given in Fig. 6d. The prepared sensor showed clear response towards the addition of DA, while the successive addition of AA and UA exhibits no response. Further addition of DA continues to elicit a response, indicating 25-fold of AA and UA over DA (simulation of real sample) hardly caused interference; and the AA and UA can not be quantified by amperometric curves under the conditions which have been selected for the determination of DA. From the obtained results, it is clear that this fabricated sensor reduced the influence of possible interfering species and exhibited an excellent selectivity towards DA.

This prepared DA sensor is comparable with previously published reports and the comparative results are shown in Table 1. The obtained detection potential, linear range and detection limit of the fabricated DA sensor is much comparable than that previously reported DA sensors. To evaluate the reliability of the prepared sensor in practical applications, the  $\text{Ag}_2\text{Se}/\text{MoSe}_2/\text{GCE}$  was used to determine DA in human serum samples. Prior to analysis, the serum samples were centrifuged for 6 min at 10000 rpm in order to remove precipitated proteins, and then were diluted 100-fold with PBS+GSH (pH 8.5). Due to low concentrations of DA in the serum, the accuracy of this method for DA detection in human serum sample was evaluated by determining the recovery of DA by addition of a known quantity of standard DA solution into the corresponding serum samples. The parallel experiment was carried

out three times. As shown in Table S1, with six different additions of DA to the serum samples, the obtained recoveries ranged from 98.00 to 103.00%. The good recovery indicates that the developed method has good accuracy and feasibility for practical analysis.

#### **4. Conclusions**

GSH as a kind of thiol tripeptide was firstly used as the polymerization inhibitor to prevent the polymerization of DA in alkaline environment. The alkaline environment is effective for reducing the energy needed during the electrooxidation of DA, lowering the oxidation peak potential of DA to 0.04 V vs. SCE in this study. Beside, Ag<sub>2</sub>Se/MoSe<sub>2</sub> was fabricated as the modified material of electrode and used for highly sensitive, selective and stable detection of DA without the matrix interference of serum sample. Under conditions optimized for the detection of DA, the linear range is from 0.05 to 1110 µM, and the lower detection limit is 9 nM. Based on the inhibition of GSH to DA polymerization in alkaline environment, sensitive and stable detection of dopamine can be achieved at pH 8.5. It provides a simple and reliable technique for DA detection in biological samples.

#### **Acknowledgments**

This work was supported by the National Science Foundation of China under Grant Nos. 51372106 and J1103307.

## Reference

- [1] G.D. Stuber, M. Klanker, B. Ridder, M.S. Bowers, R.N. Joosten, M.G. Feenstra, A. Bonci, Reward-predictive cues enhance excitatory synaptic strength onto mid brain dopamine neurons, *Science* 321 (2008) 1690-1692.
- [2] K.A. Jennings, A comparison of the subsecond dynamics of neurotransmission of dopamine and serotonin, *ACS Chem. Neurosci.* 4 (2013) 704-714.
- [3] V. Sossi, R. Fuente-Fernández, R. Nandhagopal, M. Schulzer, J. McKenzie, T.J. Ruth, J.O. Aasly, M.J. Farrer, Z.K. Wszolek, J.A. Stoessl, Dopamine turnover increases in asymptomatic LRRK2 mutations carriers, *Movement Disord.* 25 (2010) 2717-2723.
- [4] N. Jenkinson, P. Brown, New insights into the relationship between dopamine, beta oscillations and motor function, *Trends Neurosci.* 34 (2011) 611-618.
- [5] M.J. Catalán, E. Pablo-Fernández, C. Villanueva, S. Fernández-Diez, T. Lapeña-Montero, R. García-Ramos, E. López-Valdés, Levodopa infusion improves impulsivity and dopamine dysregulation syndrome in Parkinson's disease, *Movement Disord.* 28 (2013) 2007-2010.
- [6] C. Iuga, J.R. Alvarez-Idaboy, A. Vivier-Bunge, ROS initiated oxidation of dopamine under oxidative stress conditions in aqueous and lipidic environments, *J. Phys. Chem. B* 115 (2011) 12234-12246.
- [7] K.L. Tsai, Y.Y. Cheng, H.B. Leu, Y.Y. Lee, T.J. Chen, D.H. Liu, C.L. Kao, Investigating the role of Sirt1-modulated oxidative stress in relation to benign

paroxysmal positional vertigo and Parkinson's disease, *Neurobiol. Aging* 36 (2015) 2607-2616.

[8] M.J. Kim, M. Park, D.W. Kim, M.J. Shin, O. Son, H.S. Jo, H.J. Yeo, S.B. Cho, J.H. Park, C.H. Lee, D.S. Kim, O.S. Kwon, J. Kim, K.H. Han, J. Park, W.S. Eum, S.Y. Choi, Transduced PEP-1-PON1 proteins regulate microglial activation and dopaminergic neuronal death in a Parkinson's disease model, *Biomaterials* 64 (2015) 45-56.

[9] Z.D. Zhou, Y.H. Lan, E.K. Tan, T.M. Lim, Iron species-mediated dopamine oxidation, proteasome inhibition, and dopaminergic cell demise: Implications for iron-related dopaminergic neuron degeneration, *Free Radical Bio. Med.* 49 (2010) 1856-1871.

[10] K. Mcfarland, T.A. Spalding, D. Hubbard, J.N. Ma, R. Olsson, E.S. Burstein, Low dose bexarotene treatment rescues dopamine neurons and restores behavioral function in models of Parkinson's disease, *ACS Chem. Neurosci.* 4 (2013) 1430-1438.

[11] N. Bódi, S. Kéri, H. Nagy, A. Moustafa, C.E. Myers, N. Daw, G. Dibó, A. Takáts, D. Bereczki, M.A. Gluck, Reward-learning and the novelty-seeking personality: a between- and within-subjects study of the effects of dopamine agonists on young Parkinson's patients, *Brain* 132 (2009) 2385-2395.

[12] R. Burai, N. Ait-Bouziad, A. Chiki, H.A. Lashuel, Elucidating the role of site-specific nitration of  $\alpha$ -synuclein in the pathogenesis of Parkinson's disease via protein semisynthesis and mutagenesis, *J. Am. Chem. Soc.* 137 (2015) 5041-5052.

[13] Z.Q. Jia, H. Zhu, B.R. Misra, Y.B. Li, H.P. Misra, Dopamine as a potent inducer

of cellular glutathione and NAD(P)H: quinone oxidoreductase 1 in PC12 neuronal cells: a potential adaptive mechanism for dopaminergic neuroprotection, *Neurochem. Res.* 33 (2008) 2197-2205.

[14] D. Ross, J.K. Kepa, S.L. Winski, H.D. Beall, A. Anwar, D. Siegel, NAD(P)H:quinone oxidoreductase 1 (NQO1): chemoprotection, bioactivation, gene regulation and genetic polymorphisms, *Chem. Biol. Interact* 129 (2000) 77-97.

[15] E. Shimizu, K. Hashimoto, N. Komatsu, M. Iyo, Roles of endogenous glutathione levels on 6-hydroxydopamine-induced apoptotic neuronal cell death in human neuroblastoma SK-N-SH cells, *Neuropharmacology* 43 (2002) 434-443.

[16] M.F. Beal, N.Y. Ann, Mitochondria, oxidative damage, and inflammation in Parkinson's disease, *Acad Sci.* 991 (2003) 120-131.

[17] C. Voshavar, M. Shah, L.P. Xu, A.K. Dutta, Assessment of protective role of multifunctional dopamine agonist D-512 against oxidative stress produced by depletion of glutathione in PC12 cells: implication in neuroprotective therapy for parkinson's disease, *Neurotox. Res.* 28 (2015) 302-318.

[18] V. Ranc, Z. Markova, M. Hajdich, R. Prucek, L. Kvitek, J. Kaslik, K. Safarova, R. Zboril, Magnetically assisted surface-enhanced raman scattering selective determination of dopamine in an artificial cerebrospinal fluid and a mouse striatum using Fe<sub>3</sub>O<sub>4</sub>/Ag nanocomposite, *Anal. Chem.* 86 (2014) 2939-2946.

[19] M. Kaya, M. Volkan, New approach for the surface enhanced resonance raman scattering (SERRS) detection of dopamine at picomolar (pM) levels in the presence of ascorbic acid, *Anal. Chem.* 84 (2012) 7729-7735.

- [20] Y. Mao, Y. Bao, D.X. Han, F.H. Li, L. Niu, Efficient one-pot synthesis of molecularly imprinted silica nanospheres embedded carbon dots for fluorescent dopamine optosensing, *Biosens. Bioelectron.* 38 (2012) 55-60.
- [21] Y. Jie, N. Wang, X. Cao, Y. Xu, T. Li, X.J. Zhang, Z.L. Wang, Self-powered triboelectric nanosensor with poly(tetrafluoroethylene) nanoparticle arrays for dopamine detection, *ACS Nano* 9 (2015) 8376-8383.
- [22] T.O. Ahmadov, P. Joshi, J.N. Zhang, K. Nahan, J.A. Caruso, P. Zhang, Paramagnetic relaxation based biosensor for selective dopamine detection, *Chem. Commun.* 51 (2015) 11425-11428.
- [23] Y. Tao, Y.H. Lin, J.S. Ren, X.G. Qu, A dual fluorometric and colorimetric sensor for dopamine based on BSA-stabilized Au nanoclusters, *Biosens. Bioelectron.* 42 (2013) 41-46.
- [24] S.M. Wang, Z. Luo, W.P. Wang, X.G. Chen, Z.D. Hu, Simultaneous determination of dopamine, epinephrine and 5-Hydroxytryptamine in toad venom and common yam rhizome by MEKC, *Chromatographia* 70 (2009) 1467-1471.
- [25] M. Mamiński, M. Olejniczak, M. Chudy, A. Dybko, Z. Brzózka, Spectrophotometric determination of dopamine in microliter scale using microfluidic system based on polymeric technology, *Anal. Chim. Acta* 540 (2005) 153-157.
- [26] A.C. Schmidt, X. Wang, Y. Zhu, L.A. Sombers, Carbon nanotube yarn electrodes for enhanced detection of neuro-transmitter dynamics in live brain tissue, *ACS Nano* 7 (2013) 7864-7873.
- [27] Z.H. Yang, Y. Zhuo, Y.Q. Chai, R. Yuan, High throughput immunosensor based

on multi-label strategy and a novel array electrode, *Sci. Rep.* 4 (2014) 1-7.

[28] S. Sansuk, E. Bitziou, J.A. Covington, M.B. Joseph, M.G. Boutelle, P.R. Unwin, J.V. Macpherson, Ultrasensitive detection of dopamine using a carbon nanotube network microfluidic flow electrode, *Anal. Chem.* 85 (2012) 163-169.

[29] M. Lavoie, B. Ostaszewski, A. Weihofen, M. Schlossmacher, J. Selkoe, Dopamine covalently modifies and functionally inactivates parkin, *Nat. Med.* 11 (2005) 1214-1221.

[30] Wang, Y.; Li, Y.; Tang, L.; Lu, J.; Li, J. Application of grapheme modified electrode for selective detection of dopamine, *Electrochem. Commun.* 11 (2009) 889-892.

[31] L. Wang, H.R. Xu, Y.L. Song, J.P. Luo, W.J. Wei, S.W. Xu, X.X. Cai, Highly sensitive detection of quantal dopamine secretion from pheochromocytoma cells using neural microelectrode array electrodeposited with polypyrrole graphene, *ACS Appl. Mater. Interfaces* 7 (2015) 7619-7626.

[32] H. Mao, J.C. Liang, H.F. Zhang, Q. Pei, D.L. Liu, S.Y. Wu, Y. Zhang, X.M. Song, Poly(ionic liquids) functionalized polypyrrole/graphene oxide nanosheets for electrochemical sensor to detect dopamine in the presence of ascorbic acid, *Biosens. Bioelectron.* 70 (2015) 289-298.

[33] B.B. Li, Y.S. Zhou, W. Wu, M. Liu, S.R. Mei, Y.K. Zhou, T. Jing, Highly selective and sensitive determination of dopamine by the novel molecularly imprinted poly(nicotinamide)/CuO nanoparticles modified electrode, *Biosens. Bioelectron.* 67 (2015) 121-128.

- [34] Q. Wei, F.L. Zhang, J. Li, B.J. Li, C.S. Zhao, Oxidant-induced dopamine polymerization for multifunctional coatings, *Polym. Chem.* 1 (2010) 1430-1433.
- [35] J.L. Wang, B.C. Li, Z.J. Li, K.F. Ren, L.J. Jin, S.M. Zhang, H. Chang, Y.X. Sun, J. Ji, Electropolymerization of dopamine for surface modification of complex-shaped cardiovascular stents, *Biomaterials* 35 (2014) 7679-7689.
- [36] F.Y. Liu, X.X. He, J.P. Zhang, H.D. Chen, H.M. Zhang, Z.X. Wang, Controllable synthesis of polydopamine nanoparticles in microemulsions with pH-activatable properties for cancer detection and treatment, *J. Mater. Chem. B* 3 (2015) 6731-6739.
- [37] K.J. Huang, Y.J. Liu, Y.M. Liu, L.L. Wang, Molybdenum disulfide nanoflower-chitosan-Au nanoparticles composites based electrochemical sensing platform for bisphenol A determination, *J. Hazard. Mater.* 276 (2014) 207-215.
- [38] Y. Liu, M.Q. Zhu, D. Chen, Sheet-like  $\text{MoSe}_2/\text{C}$  composites with enhanced Li-ion storage properties, *J. Mater. Chem. A* 3 (2015) 11857-11862.
- [39] K.J. Huang, J.Z. Zhang, J.L. Cai, Preparation of porous layered molybdenum selenide-graphene composites on Ni foam for high-performance supercapacitor and electrochemical sensing, *Electrochim. Acta* 180 (2015) 770-777.
- [40] D.S. Kong, H.T. Wang, J.J. Cha, M. Pasta, K.J. Koski, J. Yao, Y. Cui, Synthesis of  $\text{MoS}_2$  and  $\text{MoSe}_2$  films with vertically aligned layers, *Nano Lett.* 13 (2013) 1341-1347.
- [41] K.J. Huang, H.L. Shuai, J.Z. Zhang, Ultrasensitive sensing platform for platelet-derived growth factor BB detection based on layered molybdenum selenide-graphene composites and Exonuclease III assisted signal amplification,



Biosens. Bioelectron. 77 (2016) 69-75.

[42] K.J. Huang, Y.J. Liu, J.Z. Zhang, J.T. Cao, Y.M. Liu, Aptamer/Au nanoparticles/cobalt sulfide nanosheets biosensor for  $17\beta$ -estradiol detection using a guanine-rich complementary DNA sequence for signal amplification, Biosens. Bioelectron. 67 (2015) 184-191.

[43] G.W. Shim, K. Yoo, S.B. Seo, J. Shin, D.Y. Jung, I.S. Kang, C.W. Ahn, B.J. Cho, S.Y. Choi, Large-area single-layer  $\text{MoSe}_2$  and its van der waals heterostructures, ACS Nano 8 (2014) 6655-6662.

[44] C.Y. Zeng, W.X. Zhang, S.X. Ding, Z.H. Yang, H. Zeng, Z.C. Li, Oriented attachment growth of ultra-long  $\text{Ag}_2\text{Se}$  crystalline nanowires via water evaporation-induced self-assembly, CrystEngComm 15 (2013) 5127-5133.

[45] H. Tang, K.P. Dou, C.C. Kaun, Q. Kuang, S.H. Yang,  $\text{MoSe}_2$  nanosheets and their graphene hybrids: synthesis, characterization and hydrogen evolution reaction studies, J. Mater. Chem. A 2 (2014) 360-364.

[46] L. Zhu, S. Ye, A. Ali, K. Ulla, K.Y. Cho, W.C. Oh, Modified hydrothermal synthesis and characterization of reduced graphene oxide-silver selenide nanocomposites with enhanced reactive oxygen species generation, Chinese J. Catal. 36 (2015) 603-611.

[47] X.L. Wang, Y.J. Gong, G. Shi, W.L. Chow, K. Keyshar, G. Ye, R. Vajtai, J. Lou, Z. Liu, E. Ringe, B.K. Tay, P.M. Ajayan, Chemical vapor deposition growth of crystalline monolayer  $\text{MoSe}_2$ , ACS Nano 8 (2014) 5125-5131.

[48] W.W. Xu, J.Z. Niu, H.Z. Wang, H.B. Shen, L.S. Li, Size, shape-dependent

growth of semiconductor heterostructures mediated by Ag<sub>2</sub>Se nanocrystals as seeds, ACS Appl. Mater. Interfaces 5 (2013) 7537-7543.

[49] P.N. Reddy, A. Sreedhar, M.H.P. Reddy, S. Uthanna, J.F. Pierson, The effect of oxygen partial pressure on physical properties of nano-crystalline silver oxide thin films deposited by RF magnetron sputtering, Cryst. Res. Technol. 46 (2011) 961-966.

[50] Y.C. Mao, W. Li, X.F. Sun, Y.J. Ma, J. Xia, Y.F. Zhao, X.H. Lu, J.Y. Gan, Z.Q. Liu, J. Chen, P. Liu, Y.X. Tong, Room-temperature ferromagnetism in hierarchically branched MoO<sub>3</sub> nanostructures, CrystEngComm 14 (2012) 1419-1424.

[51] W.C. Ye, D.A. Wang, H. Zhang, F. Zhou, W.M. Liu, Electrochemical growth of flowerlike gold nanoparticles on polydopamine modified ITO glass for SERS application, Electrochim. Acta 55 (2010) 2004-2009.

[52] S.B. Berman, T.G. Hastings, Dopamine oxidation alters mitochondrial respiration and induces permeability transition in brain mitochondria: Implications for Parkinson's disease, J. Neurochem. 73 (1999) 1127-1137.

[53] M.J. LaVoie, B.L. Ostaszewski, A. Weihofen, M.G. Schlossmacher, D.J. Selkoe, Dopamine covalently modifies and functionally inactivates parkin, Nat. Med. 11 (2005) 1214-1221.

[54] S. Pruneanu, A.R. Biris, F. Pogacean, C. Socaci, M. Coros, M.C. Rosu, F. Watanabe, A.S. Biris, The influence of uric and ascorbic acid on the electrochemical detection of dopamine using graphene-modified electrodes, Electrochim. Acta 154 (2015) 197-204.

## **Biographies**

Chunming Wang is a professor of chemistry, College of Chemistry and chemical engineering, Lanzhou University, China. His research interests cover electroanalytical chemistry.

Weichun Ye is an associate professor, College of Chemistry and chemical engineering, Lanzhou University, China. His current research interests cover electroanalytical chemistry and materials chemistry.

Yonglin Du is a lecturer, College of Chemistry and chemical engineering, Lanzhou University, China. Majoring in analytical chemistry and materials chemistry.

Xiaohong Xia is currently a doctor student of Lanzhou University, her research interests cover electroanalytical chemistry.

Xuan Shen is a postgraduate student of Lanzhou University currently majoring in electroanalytical chemistry and materials chemistry.

### Figure captions and table captions

Fig. 1. (a) SEM and (b) TEM images of  $\text{Ag}_2\text{Se}/\text{MoSe}_2$ . (c) HRTEM image of  $\text{Ag}_2\text{Se}/\text{MoSe}_2$ . (d) and (e) FFT patterns of the selected areas marked by frame A and B in (c). (f) XRD pattern of  $\text{Ag}_2\text{Se}/\text{MoSe}_2$ .

Fig. 2. XPS spectra of  $\text{Ag}_2\text{Se}/\text{MoSe}_2$ : (a) Mo 3d, (b) Ag 3d and (c) Se 3d. (d) XPS spectrum of O 1s.

Fig. 3. (a) Raman spectra of dopamine (bottom) and polydopamine (top). Inset is the photograph of polydopamine generated during continuously CV scanning at pH 8.5. (b) Probable mechanism of dopamine polymerization.

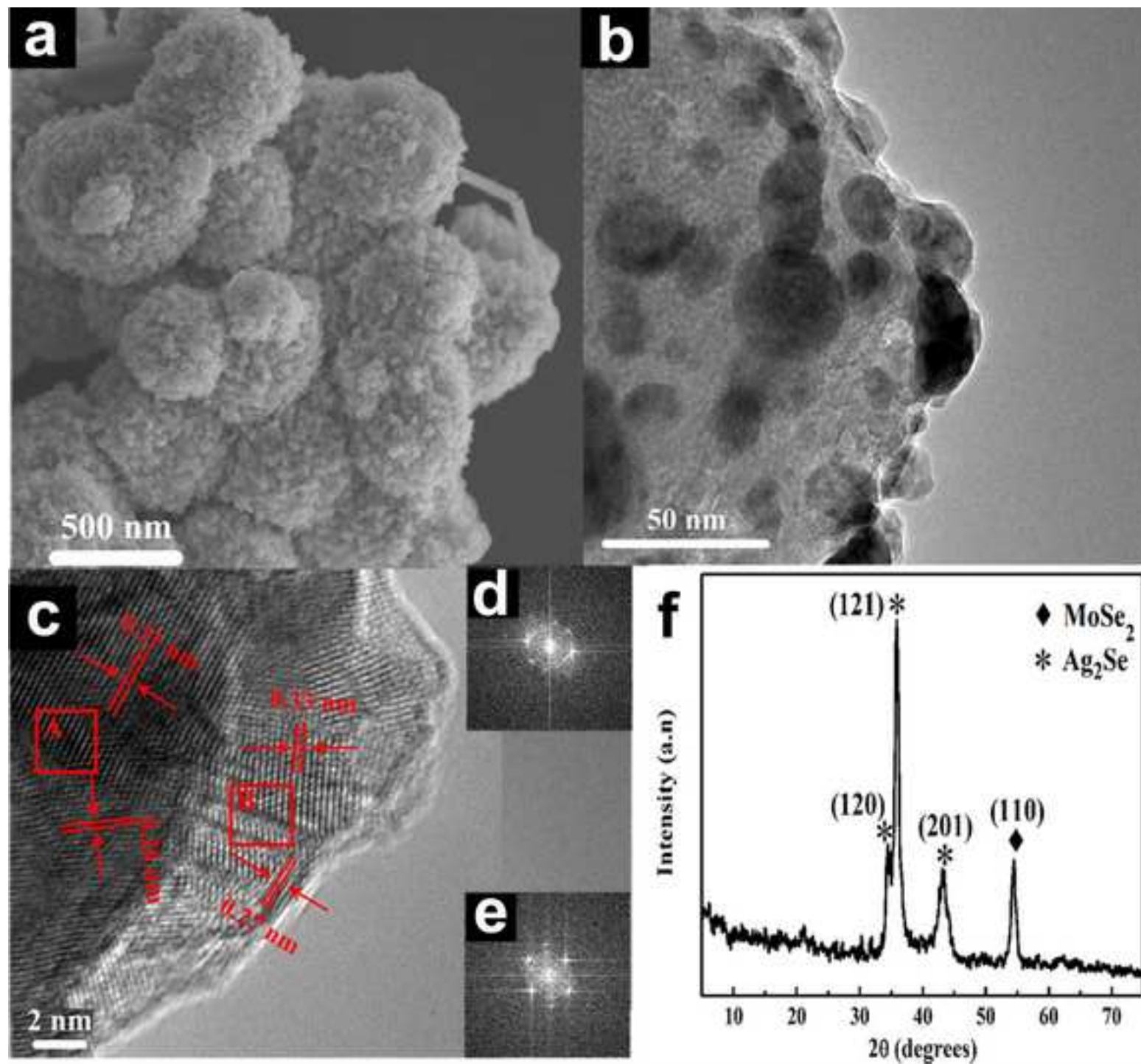
Fig. 4. (a) CVs recorded at  $\text{Ag}_2\text{Se}/\text{MoSe}_2/\text{GCE}$  in the DA solution (pH 8.5) with and without GSH. CV changes from 1st to 10th cycle of the DA solution which (b) without and (c) with GSH. Insets are the changes of solution color. (d) SEM images of the electrode surface (d) before and (e and f) after scanned in the DA solution which without (e) and with (f) GSH for 10 cycles.

Fig. 5. The probable mechanism of the oxidation of dopamine and the irreversible chemical reaction between the dopamine quinone and GSH.

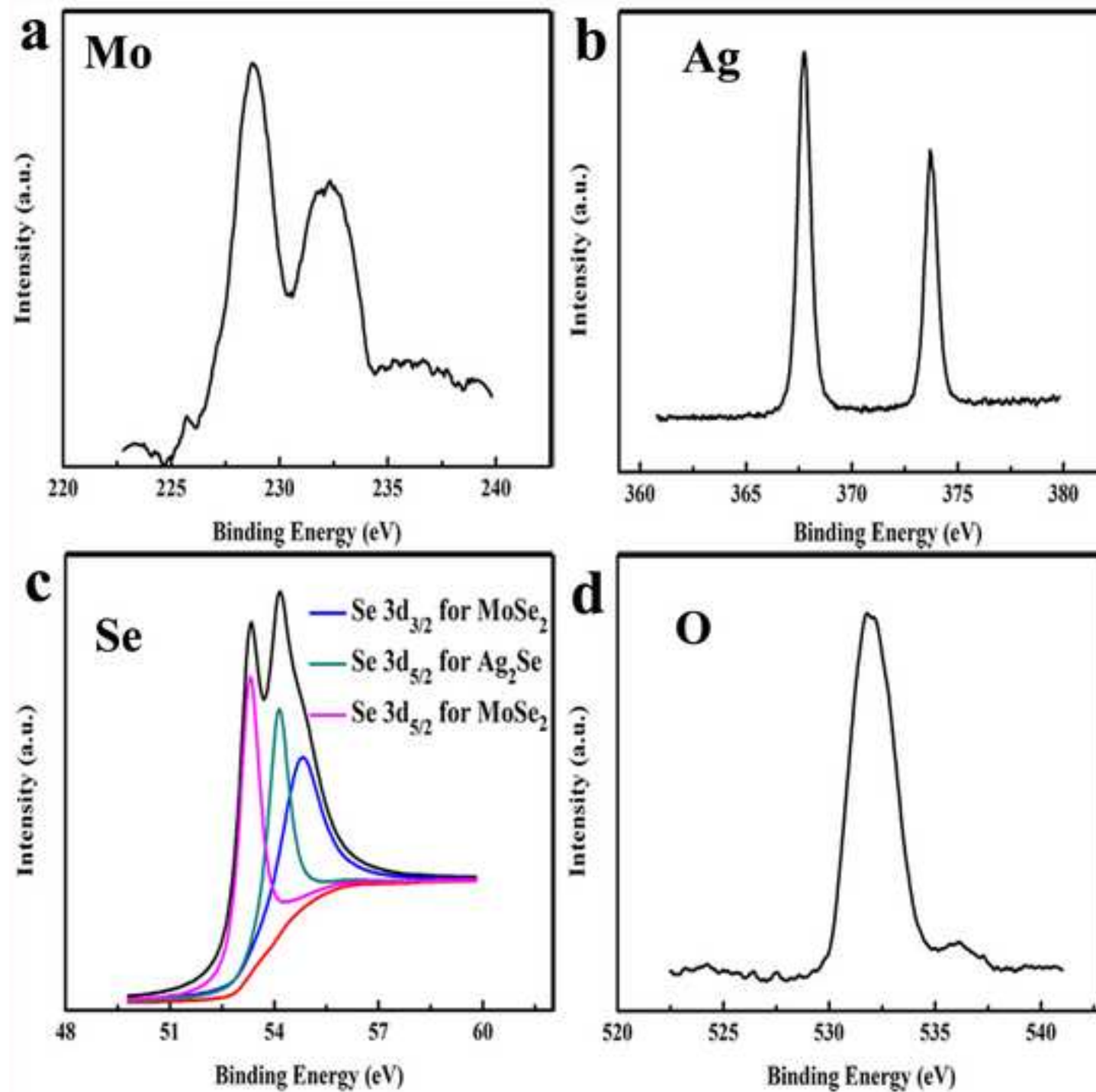
Fig. 6. Amperometric responses of  $\text{Ag}_2\text{Se}/\text{MoSe}_2/\text{GCE}$  upon the addition of 0.05 to 1110 mM dopamine in (a) PBS+GSH and (b) PBS solution (inset: amperometric responses of low concentration of DA solution). (c) Plot of  $\log C$  vs.  $\log I_{pa}$  obtained from (a). (d) Interference test of  $\text{Ag}_2\text{Se}/\text{MoSe}_2/\text{GCE}$  upon the addition of different analytes.

Table 1. Comparison of the response characteristics based on present  $\text{Ag}_2\text{Se}/\text{MoSe}_2/\text{GCE}$  and the previously reported electrochemical sensor for dopamine detection.

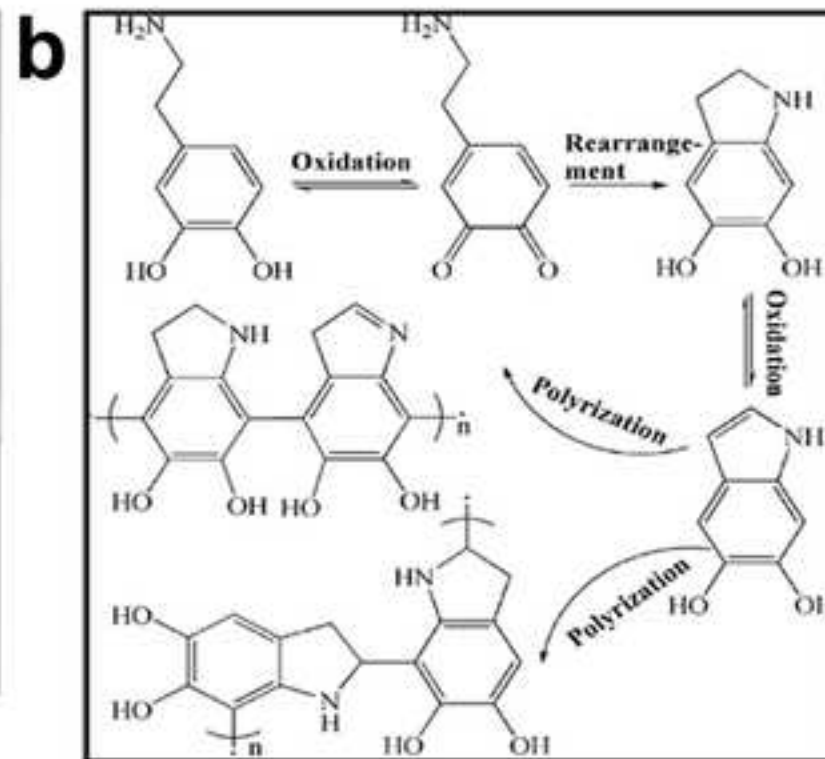
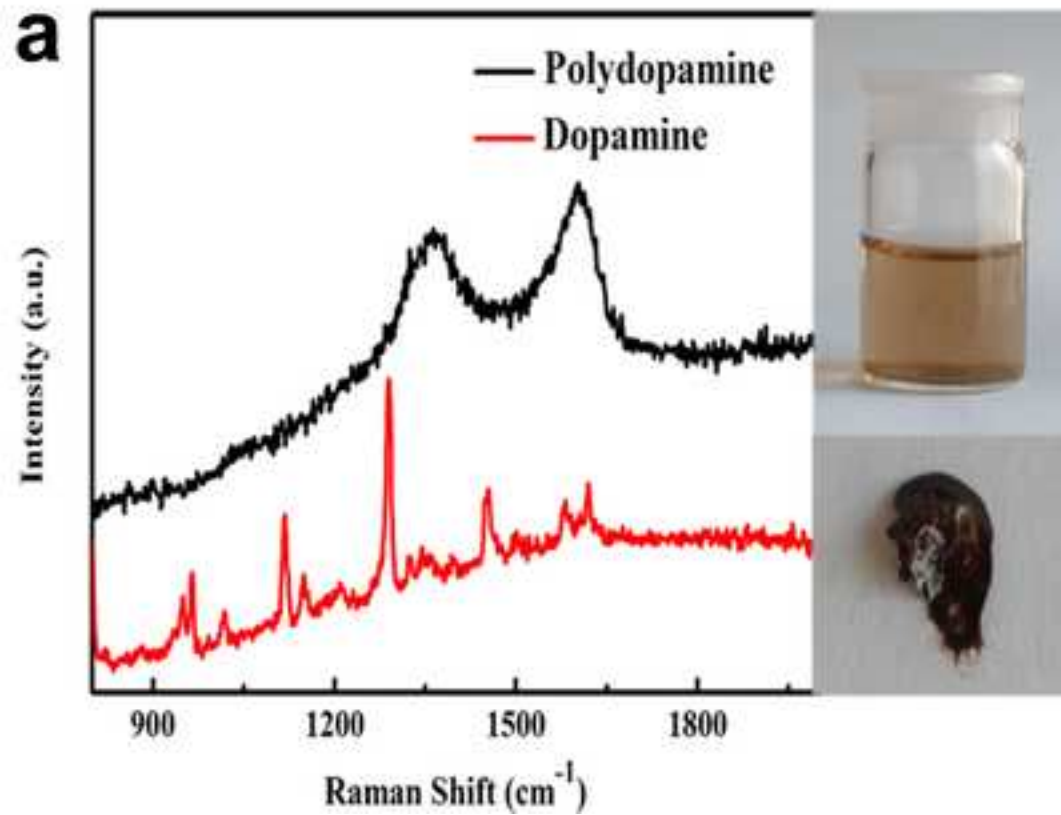
Figure(1)



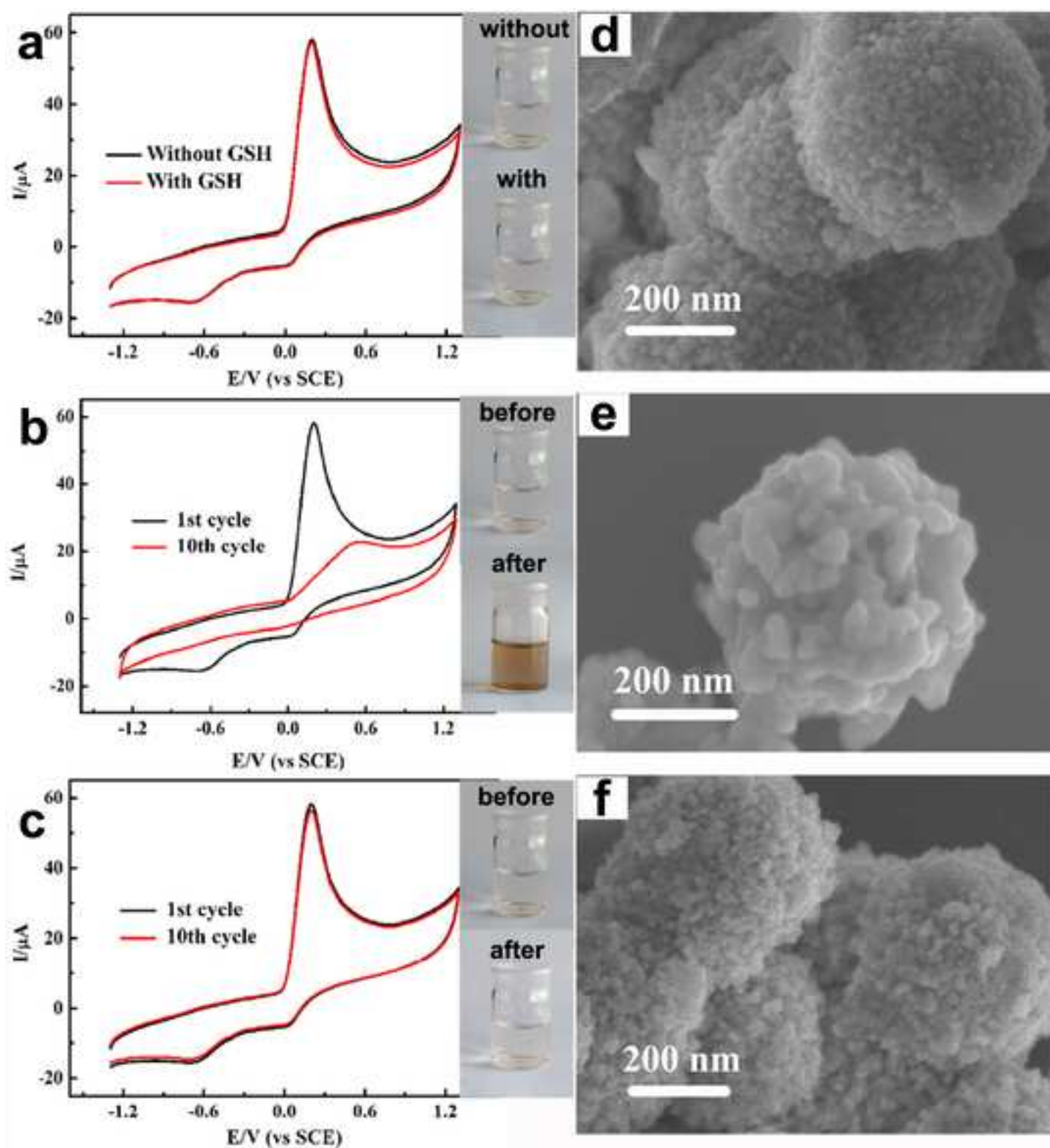
Figure(2)



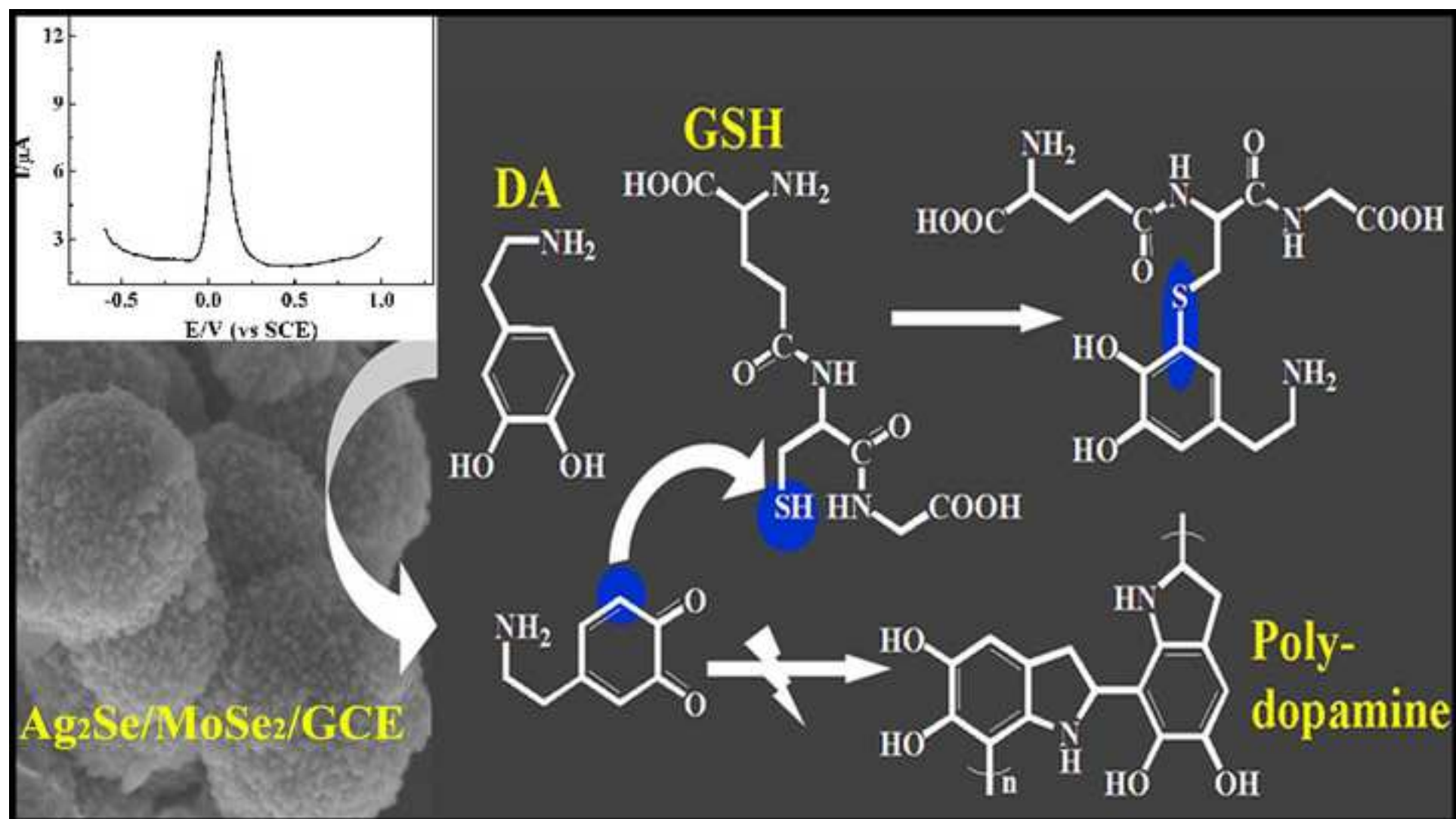
Figure(3)







Figure(5)



Figure(6)

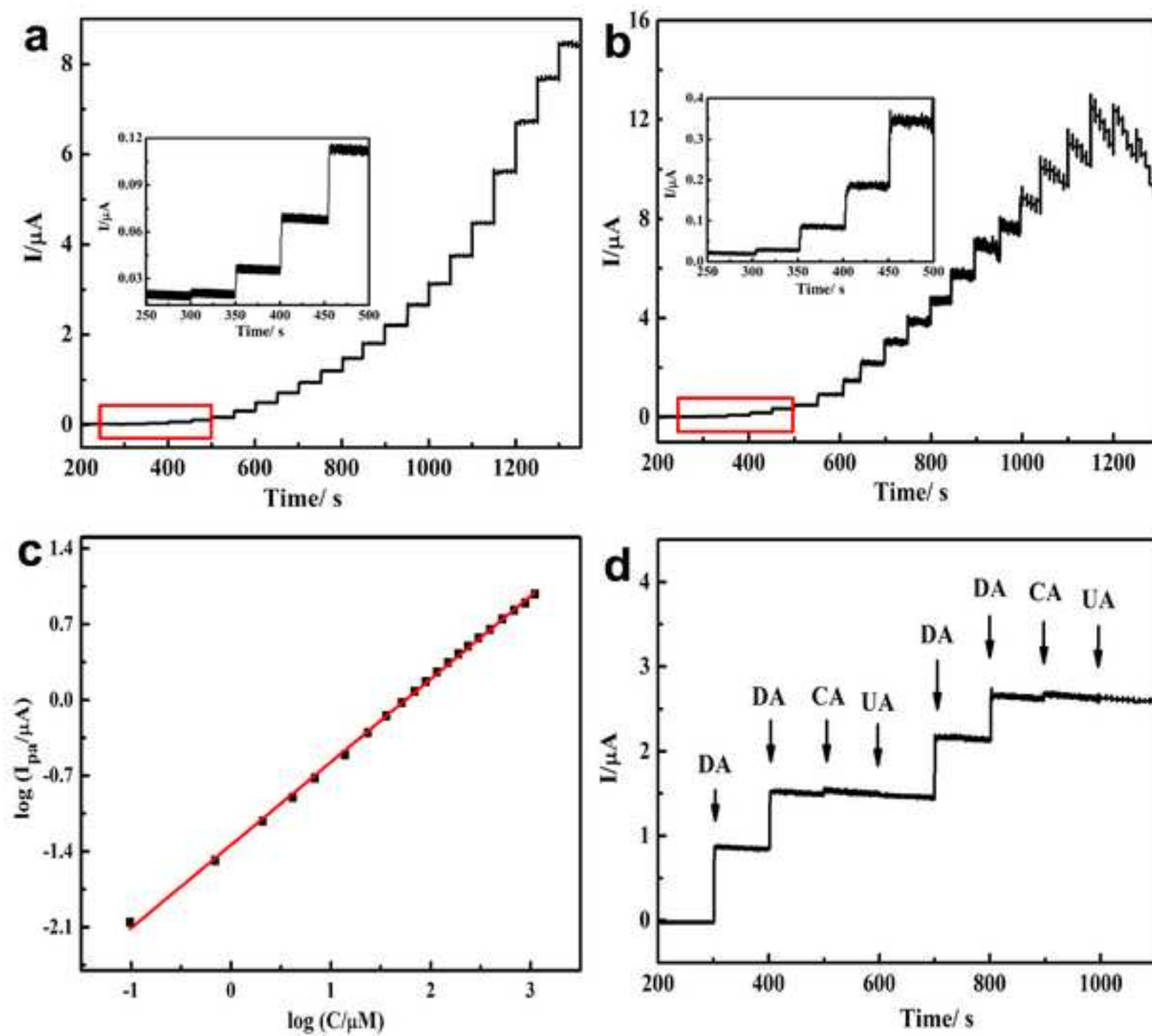


Table 1. Comparison of the response characteristics based on present Ag<sub>2</sub>Se/MoSe<sub>2</sub>/GCE and the previously reported electrochemical sensor for dopamine detection.

Electrode material	Detection method	pH	Detection potential (V)	Linear range (μM)	Detection limit (μM)	Reference
PG/nMEA <sup>[a]</sup>	Chronoamperometry	7.4	0.27	0.8-10	0.004	[31]
Au/Gr-AuAg <sup>[b]</sup>	SW	6.0	0.24	0.3-300	0.205	[54]
PILs/PPy/GO <sup>[c]</sup>	DPV	4.0	0.4	4-18	0.073	[32]
MIPs/CuO <sup>[d]</sup>	CV	7.5	0.1	0.02-25	0.008	[33]
Ag <sub>2</sub> Se/MoSe <sub>2</sub>	Chronoamperometry	8.5	0.04	0.05-1100	0.009	This work

[a] polypyrrole graphene modified neural microelectrode array(PG/nMEA).

[b] Au/Graphene-AuAg (Au/Gr-AuAg).

[c] poly(ionic liquids) functionalized polypyrrole/graphene oxide nanosheets (PILs/PPy/GO).

[d] molecularly imprinted poly(nicotinamide)/CuO. (MIPs/CuO).